

Ion-molecule charge exchange: He^+ and Ar^+ on H_2 and N_2 †

W. L. Hodge, Jr., A. L. Goldberger, M. Vedder, and E. Pollack

Department of Physics, University of Connecticut, Storrs, Connecticut 06268

(Received 10 June 1977)

Charge exchange in He^+ and Ar^+ collisions with H_2 (D_2) and N_2 is studied at small angles. This work extends our earlier studies which primarily emphasized the direct inelastic scattering at low keV energies. Using time-of-flight techniques for energy analysis of the scattered atoms, it is directly shown, for the first time, that in $\text{Ar}^+ + \text{H}_2$, $\text{Ar}^+ + \text{N}_2$, and $\text{He}^+ + \text{N}_2$ the dominant small-angle charge-exchange process is quasisonant ($Q \approx 0$). In $\text{He}^+ + \text{H}_2$ there is no available quasisonant channel, and here the dominant final channels are associated with energy losses from 13 to 18 eV. A simple model is proposed.

I. INTRODUCTION

Studies of low-keV-energy inelastic collisions in $\text{Ar}^+ + \text{N}_2$, $\text{He}^+ + \text{N}_2$, and $\text{He}^+ + \text{H}_2$ have recently been reported.^{1,2} Although these are complex systems, the results of this earlier work clearly indicated that simplifications in the theoretical treatment of such collision problems are indeed possible. As examples, it was concluded that (a) the collision occurs with the entire molecule rather than with one of its atoms, (b) only the ground and selected electronically excited states of the molecule participate in the scattering, and (c) the electronic and vibrational excitation occur independently. The last conclusion, (c), is of special interest since the collision problem becomes separable into an electronic excitation problem and one involving the vibrational excitation.

Although detailed studies were made only on the direct scattering, it was shown that charge-exchange collisions are important at small angles and dominate the scattering at the larger angles. It is particularly important to understand charge exchange (in ion-atom, ion-molecule, and in ion-surface systems), since it is an important process in obtaining high-energy neutral beams for injection into magnetically confined plasmas. Charge-exchange processes also play important roles in gaseous discharges and in astrophysics. Charge-exchange collisions have been studied using optical techniques and such experiments to date have yielded significant information on the processes involved.³⁻⁵ Although optical studies are capable of providing sufficiently high energy resolution to allow identification of some of the participating states, the measurements cannot yield information on collisions resolving to the ground state or to metastable final states. Except for a very limited number of scattered projectile-emitted photon coincidence experiments (see Ref. 5 as an example), collision studies on photons generally involve total excitation cross sections. The pres-

ent work supplements the optical studies and provides for a more detailed understanding of charge exchange.

The general features of the inelastic scattering are discussed in Refs. 1 and 2. This earlier work provided some identification of the processes participating in the direct scattering, and we now resolve several of the questions raised about charge exchange. Time-of-flight (TOF) techniques are used for energy measurements on the scattered neutral atoms resulting from the collisions. The present paper reports on small-angle charge exchange in $\text{He}^+ + \text{H}_2$, $\text{Ar}^+ + \text{N}_2$, $\text{Ar}^+ + \text{H}_2$, and $\text{He}^+ + \text{N}_2$ collisions. In the last three cases, the dominant charge-exchange processes are found to be quasisonant because of the availability of energy levels which are close in energy to the incident channel. Furthermore, in these three systems, electron capture occurs into the ground state of the scattered He or Ar atom. In $\text{He}^+ + \text{H}_2$ there is no available quasisonant channel, and our experimental results show directly for the first time that the dominant small-angle charge-exchange processes occur with energy losses of 13–18 eV. These energy losses correspond to processes yielding $\text{He}^0(1s, n \geq 2) + \text{H}^+ + \text{H}(1s)$ and $\text{H}_2^+(X^2\Sigma_g^+)$ as well as $\text{He}^0(1s^2)$ accompanied by energetic $\text{H}^+ + \text{H}(n \geq 1)$ fragments. A useful model for considering the charge-exchange process is presented.

II. EXPERIMENTAL METHODS

Except for several minor modifications required for the TOF measurements,^{6,7} the basic experimental arrangement is described in Refs. 1 and 2. Figure 1 shows the modified apparatus which now includes a set of beam pulsing plates (length 1 cm, separation 0.5 cm) and a TOF detector. Although the scattered particles pass through the electrostatic energy analyzer on their way to the TOF de-

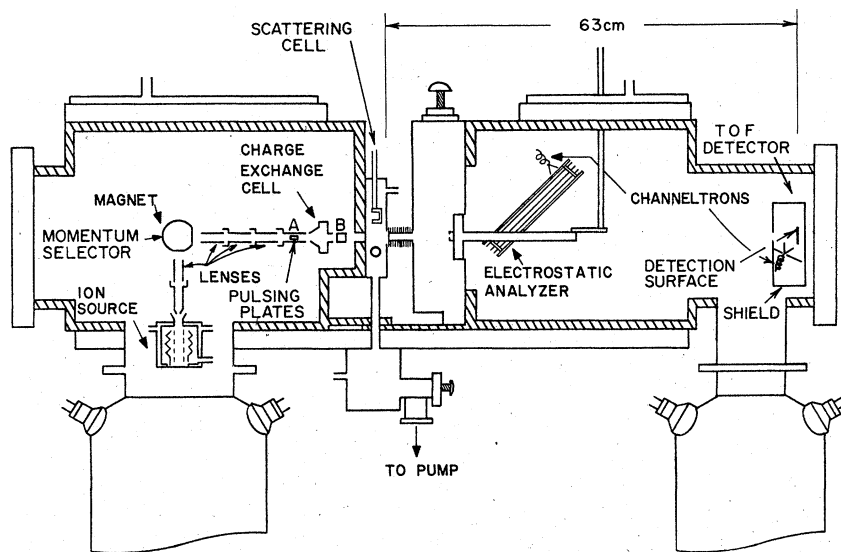


FIG. 1. Schematic of the apparatus.

detector, the analyzer is not directly used in these experiments. We do not report on scattered ions in this paper, but it is of interest to note that the TOF detector used in the present studies permits simultaneous acquisition⁸ of both the ion and neutral spectra. This is accomplished by accelerating the ions as they enter the TOF detector, thereby advancing their normal arrival time and yielding separated spectra for the ions and neutrals. The detector and related experimental techniques will be discussed in detail in future papers.⁹ For the current work, a 0.33-MHz quartz oscillator is used to trigger a signal generator which then provides a positive square-wave pulse (≈ 10 V in amplitude) to one of the pulsing plates (the second plate is biased at a fixed dc voltage). The signal generator also supplies a pulse to a single-channel analyzer

which in turn provides a delayed logic pulse to the stop input of a time-to-amplitude converter (the start pulse is provided by the detected particle). The 0–10-V output of the time-to-amplitude converter is connected to the PHA input of a multi-channel analyzer.

In an inelastic collision, ΔE , the energy loss of the scattered beam is given by

$$\Delta E = \Delta E_{e1} + Q, \quad (1)$$

where ΔE_{e1} is the kinematically required energy loss for elastic scattering at the observation angle and Q is the inelastic energy loss. In analyzing energy-loss spectra, the Q values are determined from the measured ΔE and calculated ΔE_{e1} using Eq. (1).^{1,2,7}

In the absence of elastic channels in the neutral spectra, there are no reference positions from which energy losses can directly be determined. The required positions are however established from those found from the resonant charge exchange in $\text{Ar}^+ + \text{Ar}$ and in $\text{He}^+ + \text{He}$ collisions. A typical spectrum for the $\text{Ar}^+ + \text{Ar}$ case is shown in Fig. 2. The position of the large peak corresponds to the location of the elastic reference peak, while the separation between the two peaks provides the necessary energy calibration for scattered Ar. Similar calibrations are obtained for He.

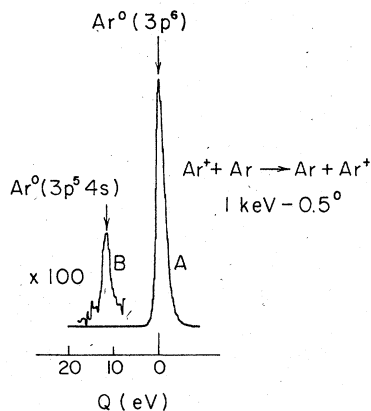


FIG. 2. Time-of-flight energy spectrum of scattered Ar^0 from 1.0-keV–0.5-deg $\text{Ar}^+ + \text{Ar}$ collisions. The energy calibration is determined from the positions of the two peaks.

III. EXPERIMENTAL RESULTS

A. $\text{Ar}^+ + \text{N}_2$

Charge exchange in $\text{Ar}^+ + \text{N}_2$ is studied at an energy of 1.0 keV and over the angular range of 0° – 2° . Figure 3 shows a typical energy spectrum of the scattered Ar^0 . The dominant peak corre-

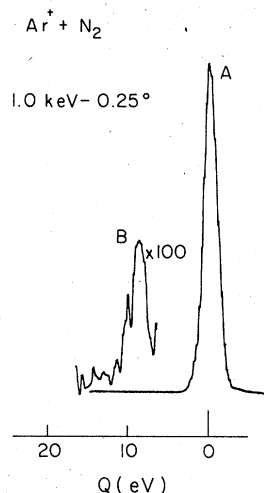


FIG. 3. Time-of-flight energy spectrum of Ar^0 from 1.0-keV-0.25-deg $\text{Ar}^+ + \text{N}_2$ collisions. Peak A corresponds to $\text{Ar}^0 + \text{N}_2^+(X^2\Sigma_g^+)$ and represents a quasisonant charge-exchange process. Peak B corresponds to $\text{Ar}^0 + \text{N}(^4S^0) + \text{N}^+(^2P)$.

sponds to a final $\text{Ar}^0 + \text{N}_2^+(X^2\Sigma_g^+)$ configuration which is in accidental energy resonance ($Q \approx 0$) with the initial $\text{Ar}^+ + \text{N}_2(X^1\Sigma_g^+)$ configuration. The spectrum also shows a weakly excited peak corresponding to $\text{Ar}^0 + \text{N}(^4S^0) + \text{N}^+(^3P)$ with $Q \approx 8.7$ eV.¹⁰

B. $\text{Ar}^+ + \text{H}_2$

The $\text{Ar}^+ + \text{H}_2$ charge-exchange collision is studied at 1.0 keV and over the angular range 0.05° to 1.25°. Figure 4 shows a typical energy spectrum of the scattered Ar^0 . The single peak corresponds to $\text{Ar}^+ + \text{H}_2 \rightarrow \text{Ar}^0 + \text{H}_2^+(X^2\Sigma_g^+)$ ($Q \approx 0$). Charge exchange in this system is dominated by this quasisonant process.

C. $\text{He}^+ + \text{N}_2$

Charge exchange in $\text{He}^+ + \text{N}_2$ is investigated at energies of 0.5 and 1.0 keV and over the angular range 0.25°–2.0°. The spectra show a single dominant peak corresponding to $\text{He}(1s^2) + \text{N}_2^+(C^2\Sigma_u^+)$ ($Q \approx 0$). This final configuration is in accidental energy resonance with the initial $\text{He}^+ + \text{N}_2(X^1\Sigma_g^+)$ configuration.

D. $\text{He}^+ + \text{H}_2$ ($\text{He}^+ + \text{D}_2$)

The $\text{He}^+ + \text{H}_2$ (and D_2) collision is studied at selected angles from 0.1° to 3.0° and at beam energies of 0.5, 0.75, and 1.0 keV. Figure 5 is an energy spectrum of the He^0 from 0.5-keV, 0.5° $\text{He}^+ + \text{D}_2$ collisions and except for the position of the peak (which moves toward larger Q values with increasing scattering angle) is typical of all

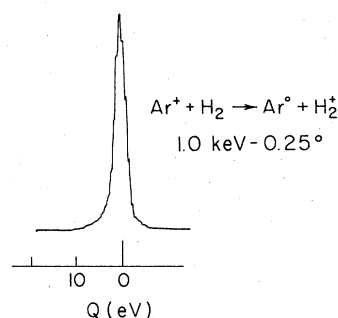


FIG. 4. Time-of-flight energy spectrum of Ar^0 from 1.0-keV-0.25-deg $\text{Ar}^+ + \text{H}_2$ collisions. The peak corresponds to $\text{Ar}^0 + \text{H}_2^+(X^2\Sigma_g^+)$ and represents a quasisonant charge-exchange process.

the spectra seen. This particular spectrum is taken with a relatively high He background pressure (in the source chamber) to locate the position from which the Q value is determined. The small peak represents resonant charge exchange in $\text{He}^+ + \text{He}$ and is independent of the H_2 scattering gas pressure. A schematic representation of the participating direct scattering states reported in Ref. 2 (and there labeled A, B, C, and D) as well as a selected number of charge exchanged states is shown in Fig. 6. As is evident, quasisonant exchange scattering is not possible since there is no state in the charge-exchange domain at the position of peak A (the elastic peak in $\text{He}^+ + \text{H}_2$). The dominant charge exchange peak in Fig. 5 has

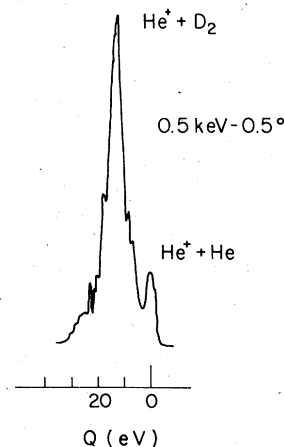


FIG. 5. Time-of-flight energy spectrum of He^0 from 0.5-keV-0.5-deg charge-exchange collisions. This spectrum is taken with a relatively high He background pressure to locate the position from which Q is determined. The small peak corresponds to resonant charge exchange in $\text{He}^+ + \text{He}$. The main peak at $Q = 13 \pm 1$ eV is at an energy loss corresponding to $\text{He}^+ + \text{D}_2 \rightarrow \text{He}^+ + \text{D}^+ + \text{D}(1s)$, as well as to $\text{He}^0(1s^2)$ accompanied by energetic $\text{D}^+ + \text{D}(n \geq 1)$. The weak structure to the left of the $\text{He}^+ + \text{He}$ peak suggests electron capture to $\text{He}(1s^2)$ at threshold Q .

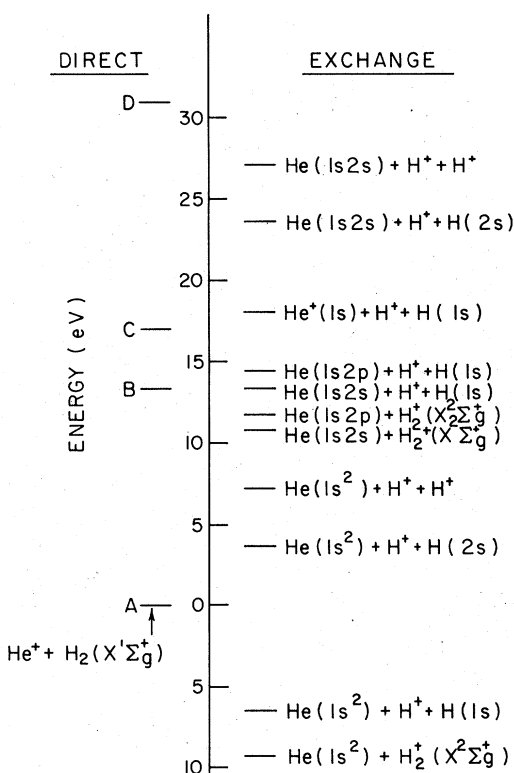


FIG. 6. Selected states in He⁺+H₂. The exchange states are shown at threshold (H⁺ and H fragments have no kinetic energy). A, B, C, and D refer to levels seen in the direct scattering reported in Ref. 2. The dominant charge-exchange processes at small angles occur with energy losses near B. This suggests electron capture into excited He levels or into He⁰(1s²) accompanied by H⁺+H(*n* ≥ 1) fragments with the necessary additional kinetic energy.

a maximum at $Q \approx 13$ eV and lies close to an excited He level. Over the entire energy and angular range studied the dominant final channels are associated with $13 \leq Q \leq 18$ eV corresponding to He⁰(1s, *n* ≥ 2) + H⁺ + H(1s) as well as to He⁰(1s²) accompanied by H⁺ + H(*n* ≥ 1) fragments with the necessary additional kinetic energy. The latter type of process can result from the excitation of an antibonding state in H₂⁺ yielding energetic dissociation fragments.

IV. DISCUSSION OF THE RESULTS

In the Ar⁺+N₂, He⁺+N₂, and Ar⁺+H₂ cases it is established that the small-angle (large-impact-parameter) charge-exchange collisions primarily involve final states corresponding to quasiresonant

($Q \approx 0$) processes. In He⁺+H₂ a quasiresonant channel is not available, and the dominant electron capture does not involve processes with the minimum allowed Q values. Within the energy resolution of the current experiment the initial small-angle charge-exchange process is peaked at $Q \approx 13$ eV. In the direct scattering studies in He⁺+H₂, the lowest electronically excited channel (peak B in Ref. 2) corresponded to a Q value of 13.3 eV. The reduced differential cross section when plotted as a function of τ , the reduced scattering angle, showed a maximum at 3 keV deg for peak B. The reduced differential cross section for charge exchange showed a maximum at the same position.² This behavior suggested that a common primary mechanism may be responsible for both peak B in the direct inelastic scattering and for the charge exchange at these angles.¹¹ The measured Q for the small-angle charge exchange provides additional justification for this interpretation and suggests a simple model of the collision which is similar to one used in explaining ion-atom charge exchange in He⁺+Ne,¹² and in the nonsymmetrical alkali ion-alkali atom cases.¹³ In these systems, the charge exchange proceeds via couplings between initial and final states that lie close together at large internuclear separation.¹⁴⁻¹⁶ In He⁺+H₂, a similar situation could exist following the collisional excitation of peak B at $Q = 13.3$ eV (as one example). Here, as the collision partners separate, this state comes close in energy to a number of exchange states resulting in possible electron transitions to them. After excitation of an exchange state, additional interactions with the direct (peak B) and other exchange states occur. In He⁺+H₂, the large number of available states results in a dominant role for charge exchange in comparison with the direct scattering.² On the basis of this model, the peaks of the reduced differential cross sections for the exchange and direct scattering will be found at a common τ value since both processes result from a common primary interaction.

A similar model could account for charge exchange in the Ar⁺+N₂, Ar⁺+H₂, and He⁺+N₂ cases. Here quasiresonant processes are possible and couplings between the direct elastic and charge-exchange channels occur. It is also interesting to note that the lowest-lying direct inelastic scattering peak in Ar⁺+N₂ is associated with a $Q = 8.1$ eV. Figure 3 shows a small peak representing Ar⁺+N₂ → Ar⁰+N(4S⁰)+N*(3P) ($Q \approx 8.7$ eV) and suggests a coupling between the direct inelastic and the close-lying charge-exchanged channel. This result is especially interesting since the observed channels occur at $Q \approx 0$ and $Q \approx 8.7$ eV while a number of other possible exchange channels with inter-

mediate Q values are not populated.

The matching of energy levels in the direct and charge-exchange cases plays an important role in determining the states excited in these collisions.

If the direct scattering state is close in energy to a large number of charge-exchanged states, they should become very important in the collision process.

‡Supported by the U. S. Army Research Office-Durham and the University of Connecticut Research Foundation.

¹S. M. Fernandez, F. J. Eriksen, A. V. Bray, and E. Pollack, Phys. Rev. A 12, 1252 (1975).

²A. V. Bray, D. S. Newman, and E. Pollack, Phys. Rev. A 15, 2261 (1977).

³R. C. Isler and R. D. Nathan, Phys. Rev. A 6, 1036 (1972).

⁴G. H. Dunn, R. Geballe, and D. Pretzer, Phys. Rev. 128, 2200 (1962).

⁵F. J. Eriksen and D. H. Jaecks, Phys. Rev. Lett. 36, 1491 (1976).

⁶J. C. Brenot, D. Dhuicq, J. P. Gauyacq, J. Pommier, V. Sidis, M. Barat, and E. Pollack, Phys. Rev. A 11, 1245 (1975).

⁷Q. C. Kessel, E. Pollack, and W. W. Smith, in *Collisional Spectroscopy*, edited by R. G. Cooks (Plenum,

New York, to be published), Chap. 2.

⁸A. L. Goldberger, D. S. Newman, M. Vedder, and E. Pollack, Bull. Am. Phys. Soc. 22, 115 (1977).

⁹A. L. Goldberger, D. S. Newman, M. Vedder, and E. Pollack (unpublished).

¹⁰F. Gilmore, J. Quant. Spectrosc. Radiat. Transfer 5, 369 (1965).

¹¹A. V. Bray, Ph.D. thesis (University of Connecticut, 1976) (unpublished).

¹²S. Nagy, S. M. Fernandez, and E. Pollack, Phys. Rev. A 3, 280 (1971).

¹³J. Perel and H. L. Daley, Phys. Rev. A 4, 162 (1971).

¹⁴R. E. Olson, Phys. Rev. A 6, 1822 (1972).

¹⁵Y. Demkov, Sov. Phys.-JETP 18, 138 (1964).

¹⁶M. Barat, J. C. Brenot, D. Dhuicq, J. Pommier, V. Sidis, R. E. Olson, E. J. Shipsey, and J. C. Browne, J. Phys. B 9, 269 (1976).